NATIONAL ADVISORY COMMITTEE FOR AERONAUTICS

TECHNICAL NOTE 1922

TWO-DIMENSIONAL INVESTIGATION OF FIVE RELATED NACA AIRFOIL

SECTIONS DESIGNED FOR ROTATING-WING AIRCRAFT

By Raymond F. Schaefer, Laurence K. Loftin, Jr.,
and Elmer A. Horton

Langley Aeronautical Laboratory
Langley Air Force Base, Va.

NACA

Washington
July 1949

NATIONAL ADVISORY COMMITTEE FOR AERONAUTICS

TECHNICAL NOTE 1922

TWO-DIMENSIONAL INVESTIGATION OF FIVE RELATED NACA AIRFOIL

SECTIONS DESIGNED FOR ROTATING-WING AIRCRAFT

By Raymond F. Schaefer, Laurence K. Loftin, Jr.,
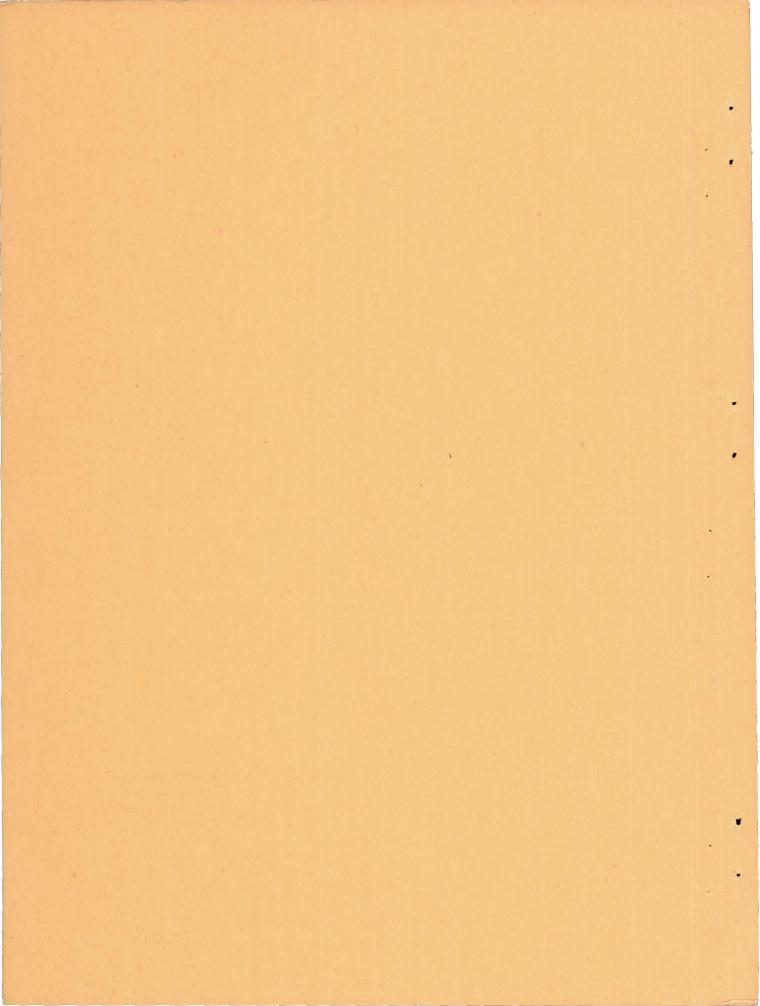and Elmer A. Horton

SUMMARY

Five NACA airfoil sections intended for use in rotor blades have
been designed and tested in the Langley two-dimensional low-turbulence
tunnel. The airfoils have thicknesses that vary from 9 percent to
15 percent of the chord and theoretical design lift coefficients that
vary from 0.3 to 0.7. Theoretical-pressure-distribution data and the
measured two-dimensional aerodynamic characteristics at Reynolds numbers
from 0.9×10^6 to 2.6×10^6 are presented for each airfoil. The effects
of surface condition were investigated at a Reynolds number
of 2.1×10^6. The results are analyzed to show the effects of vari-
ations in thickness and camber upon the pertinent section aerodynamic
characteristics. Theoretical calculations for different flight condi-
tions are also included to indicate the relative performance of sample
rotors employing the different airfoils. These calculations show that
the 9-percent-thick section of 0.5 design lift coefficient is, in
general, the best of the airfoils of the present investigation for the
flight conditions considered, but, as compared with the NACA 8-H-12
airfoil section designed in a previous NACA investigation, this section
does not appear to offer any hope of gains in performance for most of
the flight conditions.

INTRODUCTION

Studies of rotating-wing aircraft have indicated that sizable
reductions in the profile-drag power should be realized through the use
of airfoil sections designed to take advantage of the low profile-drag
coefficients associated with the attainment of relatively large extents
of laminar flow. For rotor-blade applications, low values of drag are
desirable not only at low and moderate lift coefficients but also at
high lift coefficients and, therefore, the low drag corresponding to
extensive laminar flow should be obtained at relatively high lift
coefficients. Of primary importance in all cases, however, is the

maintenance of near-zero pitching moments throughout the useful lift-coefficient range. These requirements indicate the desirability of employing cambered airfoils for rotor blades but, at the same time, preclude the use of NACA 6-series, or low-drag, airfoils (reference 1) cambered with conventional mean lines such as the a = 1.0.

Several investigations have therefore been made for the purpose of obtaining laminar-flow airfoils that have the previously mentioned desirable characteristics. The drag at high lift coefficients, the sensitivity of the airfoil to surface roughness, and the critical Mach number were other characteristics considered in the design of the airfoils. In all cases, the airfoils designed consisted of NACA 6-series basic thickness forms cambered with various specially designed mean lines.

The purpose of the initial investigation, described in reference 2, was to explore the possibility of designing sections with zero pitching moments and high maximum lift-drag ratios corresponding to the attainment of extensive laminar flow at relatively high lift coefficients. Near-zero pitching moments were obtained with the new airfoils and, in comparison with other airfoils considered for use in rotor blades, considerable improvement in the values of maximum lift-drag ratio was obtained. The new airfoils (reference 2), however, seemed to be unduly sensitive to surface roughness and were characterized by undesirable variations in the drag, lift, and moment at high lift coefficients.

In an attempt to minimize the undesirable characteristics of the airfoils discussed in reference 2, four new experimental sections were derived and tested (reference 3). Some of the airfoils described in reference 3 have highly desirable over-all characteristics and at the present time one of these airfoils, the NACA 8-H-12, is being considered for application in numerous helicopter designs. In order to allow the designer more latitude in the selection of airfoils for rotor blades, however, the evaluation of the effects of airfoil thickness and camber upon the characteristics of airfoils generally similar in design to the best of those discussed in reference 3 seemed desirable. Five airfoil sections have accordingly been derived and tested in an effort to show the effects on the aerodynamic characteristics of systematically varying the thickness and camber. The purpose of the present paper is to present pertinent design information and experimental aerodynamic characteristics of these airfoils.

The airfoils considered varied in thickness from 9 to 15 percent of the chord and in camber from 0.3 to 0.7 design lift coefficient. The NACA 64-series basic thickness form was employed for all the airfoils. The two-dimensional lift, drag, and pitching-moment characteristics were obtained for each smooth airfoil at Reynolds numbers of approximately 0.9×10^6, 2.1×10^6, and 2.6×10^6. The effects upon

the aerodynamic characteristics of roughening the leading edges of the
models were determined at a Reynolds number of 2.1×10^6. In conjunc-
tion with the analysis of the airfoil characteristics obtained, an
evaluation has been made according to the methods of reference 4 of the
performance characteristics under various flight conditions to be
expected from rotors employing the different airfoils.

SYMBOLS

Airfoil-Section Symbols

a	mean-line designation, fraction of chord from leading edge over which design load is uniform
α_o	section angle of attack
c	chord
c_d	section drag coefficient
$c_{d_{min}}$	minimum section drag coefficient
c_l	section lift coefficient
$c_{l_{max}}$	maximum section lift coefficient
c_{l_i}	design section lift coefficient
$(c_l/c_d)_{max}$	maximum lift-drag ratio
$c_{m_{ac}}$	section moment coefficient about aerodynamic center
$c_{m_{c/4}}$	section moment coefficient about quarter-chord point
M_{cr}	critical Mach number
R	Reynolds number
t	airfoil thickness
V	free-stream velocity
v	local velocity
x	distance along chord from leading edge

y   distance perpendicular to chord

Rotating-Wing-Aircraft Symbols

C_P power coefficient $\left(\dfrac{\text{Rotor-shaft power input}}{\rho\Omega^3\pi R^5}\right)$

α_r angle of attack of blade element from zero lift

α rotor angle of attack; angle between projection in plane
            of symmetry of axis of no feathering and line perpen-
            dicular to flight path, positive when axis is pointing
            rearward, radians

R   rotor-blade radius

V   forward speed

W/S   rotor disk loading, pounds per square foot

f   parasite drag area, square feet

λ inflow ratio $\left(\dfrac{V\sin\alpha - v'}{\Omega R}\right)$

v' induced inflow velocity at rotor

μ tip-speed ratio $\left(\dfrac{V\cos\alpha}{\Omega R}\right)$

σ rotor solidity; ratio of total blade area to swept-
            disk area (rectangular blades)

θ pitch angle of blade element

θ_1 difference between hub and tip pitch angles, degrees
            (positive when tip angle is greater)

Ω rotor angular velocity, radians per second

ρ air density

THEORETICAL AIRFOIL CHARACTERISTICS

The five airfoil sections that were derived and tested are
designated as follows:

	NACA 12-H-12	
NACA 11-H-09	NACA 13-H-12	NACA 15-H-15
	NACA 14-H-12	

The first number in the designation is a serial number, the H indi-
cates that the airfoil section has been designed for use on rotating-
wing aircraft, and the last two digits represent the magnitude of the
maximum thickness in percent of the chord. The NACA 12-H-12, 13-H-12,
and 14-H-12 sections are 12-percent-thick airfoil sections with the
amount of camber varied to give theoretical design lift coefficients
of 0.3, 0.5, and 0.7, respectively. The NACA 11-H-09, 13-H-12,
and 15-H-15 airfoil sections have the same design lift coefficient (0.5)
but have maximum thicknesses of 9, 12, and 15 percent of the chord,
respectively. The thickness forms of all the airfoils were of the
NACA 64-series (reference 1).

The mean camber line of each section was obtained by
combining a = 0, a = 0.4 (modified), and a = 1.0 mean lines. These
mean lines were combined to give first-approximation-zero, theoretical,
quarter-chord pitching moments and extensive favorable pressure
gradients along the lower surface. The design lift coefficients of the
airfoil sections in the group representative of varying amounts of
camber were obtained by linearly scaling the mean-line ordinates. The
airfoils that have the same amount of camber but different thickness
ratios, however, have mean lines that are slightly different for each
thickness ratio. These differences arise as a result of an attempt to
make the pressure distribution of the resultant cambered airfoil more
desirable for each thickness ratio than could have been obtained by
using exactly the same mean line in all cases. The loading typical of
the mean lines employed is given in figure 1 for the mean line used in
the NACA 13-H-12 section. Ordinates for the five airfoil sections are
given in tables I to V and the section profiles can be seen in
figures 2 to 6.

Calculated pressure distributions at the theoretical design lift
coefficient for each airfoil are presented in figures 2 to 6.
Increasing the airfoil thickness from 9 to 15 percent of the chord while
maintaining a constant design lift coefficient of 0.5 increases the peak
negative pressure somewhat and makes the pressure gradient on the
forward part of the upper surface more favorable for laminar flow
(figs. 2, 4, and 6). Increasing the design lift coefficient from 0.3
to 0.7 while maintaining a constant thickness of 12 percent of the chord

causes large increases in the peak negative pressure coefficient and makes the pressure gradient over the forward part of the upper surface progressively more unfavorable to the maintenance of laminar flow (figs. 3, 4, and 5). The pressure gradient on the lower surface may be seen to be favorable over the entire chord for all the airfoils and to become progressively more favorable as the camber is increased.

Although experimental pressure distributions are not available for the airfoils under consideration, previous experience with airfoils designed to produce appreciable loads near the trailing edge (reference 5) indicates that the effects of viscosity are such that the theoretical loading is not completely realized near the trailing edge. As a consequence, some of the experimentally determined characteristics of the NACA H-series airfoils would be expected to be somewhat different from those predicted on the basis of a theoretical inviscid flow. In the design of the airfoils, however, the amount of loss in load near the trailing edge was estimated and allowed for in such a way that the experimentally determined pitching moments would be expected to be near zero.

The critical Mach number M_{cr} for each airfoil section was estimated by employing the Von Kármán-Tsien relationship in which the theoretical low-speed peak negative pressure coefficients at the theoretical design lift coefficient are used; the values of M_{cr} are given in table VI. In order to give some indication of the large reduction in the theoretical values of M_{cr} produced by the addition of camber to the symmetrical sections, comparative theoretical values of the critical Mach number for the symmetrical thickness forms are also included in table VI. As would be expected, decreases in the critical speed accompany increases in camber and thickness. In view of the expected departure of the theoretical and experimental low-speed pressure distributions and the differences that usually exist between the theoretical critical and force-break Mach numbers, the practical value of the critical Mach numbers presented seems questionable.

MODELS AND TESTS

Each of the two-dimensional models that was tested in this investigation had a 24-inch chord and a $35\frac{1}{2}$-inch span and was constructed of chordwise, mahogany laminations. The models were prepared for testing by applying a thin coat of glazing compound to the surfaces and sanding in a chordwise direction with No. 400 carborundum paper until the surfaces were aerodynamically smooth. For tests with transition fixed forward at the leading edge, standard roughness was applied on the top and bottom surfaces spanwise along the leading edge of each

model over a surface length of 8 percent of the chord measured from the leading edge. A more detailed description of the standard roughness selected for 24-inch-chord models is given in reference 1.

The models were tested in the Langley two-dimensional low-turbulence tunnel. This tunnel was designed to test models completely spanning the width of the tunnel in two-dimensional flow. The rectangular test section of this closed-throat, continuous tunnel is 3 feet wide and $7\frac{1}{2}$ feet high. The turbulence level amounts to only a few hundredths of 1 percent and is achieved by the large contraction ratio (19.6 to 1) and by the use of seven layers of fine-wire, small-mesh, turbulence-reducing screens in the widest part of the entrance cone. The maximum velocity of this wind tunnel is approximately 155 miles per hour which gives a Reynolds number of about 1.4×10^6 per foot of model chord.

Lift forces and pitching moments were measured on balances and drag forces were obtained with a wake-survey apparatus. The wake-survey method was used because it had been proved to yield greater accuracy in the range of low and moderate drags than the tunnel drag balance.

The models were supported in the tunnel at the chordwise quarter-chord position, but, for structural reasons, different vertical distances were necessary between the chord line and the pitch axis of rotation for each model. All pitching moments were measured about the axis of rotation but were corrected to the true quarter-chord axis before presentation. When the models were mounted for lift and moment tests, a small gap (approx. 0.020 in.) was, of necessity, allowed between the ends of the model and the tunnel walls in order to insure freedom of the balance. Comparative low-turbulence-tunnel tests of various airfoils with and without gaps indicated that error due to leakage through these gaps is substantially within the experimental accuracy of the test methods at Reynolds numbers corresponding to the present tests. A more complete description of the tunnel and the methods of obtaining and reducing the data are given in reference 6.

Lift, drag, and pitching moments were obtained at Reynolds numbers of approximately 0.9×10^6, 2.1×10^6, and 2.6×10^6 for each airfoil in a smooth condition and at a Reynolds number of 2.1×10^6 for each airfoil with standard leading-edge roughness.

RESULTS

The results of the tests are presented (figs. 7 to 11) in the form of standard coefficients representing the lift, drag, and pitching

moment (about both the quarter chord and the aerodynamic center) at the Reynolds numbers covered for the smooth and rough surface conditions. The aerodynamic-center locations that were calculated for both surface conditions at the corresponding Reynolds numbers of the tests are also given in these figures. All the data have been corrected for the finite size of the tunnel test section. The relative magnitude of each correction is given for the NACA 11-H-09 airfoil section by the following equations (see reference 6) in which the primed symbols are the measured quantities:

$$c_l = 0.980c_l'$$

$$c_d = 0.995c_d'$$

$$c_{m_c}/4 = 0.995c_{m_c}/4'$$

$$\alpha_o = 1.015\alpha_o'$$

Corrections for the other airfoil sections are of a similar order of magnitude.

A summary of the more important aerodynamic characteristics of the five airfoils is given in table VI for both smooth and rough surface conditions and two Reynolds numbers. Included for comparison are values for the NACA 23012 and 8-H-12 airfoil sections taken from references 1 and 3, respectively.

DISCUSSION

The discussion is concerned with an analysis of the effects of variations in airfoil design upon the aerodynamic characteristics of the airfoil sections and, of perhaps greater practical importance, with the performance of helicopter rotors employing the different airfoil sections tested. The section aerodynamic characteristics considered are: pitching moment, lift, and drag.

Pitching Moment

The values of pitching moment about the aerodynamic center for all the airfoil sections are essentially constant and nearly zero throughout the useful range of lift (figs. 7 to 11). Only small changes in the aerodynamic-center pitching moments in the useful range of lift occur as a result of variations in the Reynolds number and surface

condition. No consistent variation of the chordwise position of the aerodynamic center with camber and thickness appears to exist. The range in which the values of the aerodynamic-center pitching moments remain almost constant and the positions of the aerodynamic center are summarized in table VI.

Lift

Maximum lift.- A comparison of maximum lift coefficients at Reynolds numbers of 2.1×10^6 and 2.6×10^6 for both airfoil surface conditions is given in the table of aerodynamic characteristics (table VI). The data for both Reynolds numbers indicate that the maximum section lift coefficients for all the airfoil sections in the smooth condition, including the NACA 8-H-12 section, are of the order of 1.3, except for a value nearly one-tenth higher attained by the highest-cambered airfoil, the NACA 14-H-12. The values of the maximum lift obtained at a Reynolds number of 0.9×10^6 (figs. 7 to 11) are somewhat lower than those corresponding to the higher Reynolds numbers, but the magnitude of this scale effect is relatively insignificant. Variations in thickness are seen to have little effect on the maximum lift coefficients of these airfoils and only the highest amount of camber produced an increase in the maximum lift. The effect of adding the type of camber employed in these airfoils to the symmetrical NACA 64-series sections (data for which are presented in reference 1) resulted in reductions in maximum lift coefficient for the 12-percent-thick and 15-percent-thick airfoil sections in contrast to an increase obtained with the 9-percent-thick airfoil. The maximum lift coefficients of all the airfoils considered in the present investigation and that of the NACA 8-H-12 section at a Reynolds number of 2.6×10^6 are lower than the value of 1.6 obtained for the NACA 23012 section at a Reynolds number of 3×10^6 (references 1 and 3). The type of stall shown by the NACA 23012 section is, however, much more abrupt than that which is characteristic of the H-series helicopter-rotor-blade sections.

The effect of standard leading-edge roughness is to decrease the maximum lift of all the airfoils. The magnitude of the decrement, however, varies from a value of approximately 0.1 for the NACA 11-H-09, 12-H-12, and 13-H-12 airfoil sections to 0.3 for the NACA 14-H-12 and 15-H-15 sections. The resultant maximum lift coefficients vary from 1.19 for the 9-percent-thick section to 1.04 for the 15-percent-thick section. The maximum lift coefficient of the NACA 8-H-12 section in the rough condition is also of the order of 1.1. Unpublished data show that the maximum lift of the NACA 23012 section under similar conditions is about 1.15 and that the stall is still abrupt; whereas the H-series sections in the rough condition have a more gradual type of stall just as occurred in the smooth condition.

Lift-curve slope.- The experimental data (figs. 7 to 11) for the
NACA H-series sections indicate the variation of the lift curves from a
straight line to be such that the lift-curve slopes are quite difficult
to define adequately in many cases. In order to give some indication
of their order of magnitude, however, values of the lift-curve slope
were measured for a short range of lift coefficient surrounding the
experimental design values for a Reynolds number of 2.6×10^6. For the
smooth surface condition, the lift-curve slopes so determined showed a
wide variation from values of the order of 0.100 for the 9-percent-
thick section to 0.120 for the thicker, more highly cambered airfoils.
In comparison, the theoretical value of the lift-curve slope, as shown
by thin-airfoil theory, is 2π per radian or 0.110 per degree.
Reductions in the Reynolds number generally caused some decrease in the
lift-curve slope, and, in all cases, large decreases occurred when the
leading edges of the airfoils were roughened.

Angle of zero lift.- As would be expected from theory, the angles
of zero lift are seen to become progressively more negative as the
amount of camber is increased. A small negative shift in the angle of
zero lift also occurs as the thickness ratio is increased. This small
shift may possibly be explained by the fact that as the thickness is
increased, the pressure-recovery gradients over the rear of the airfoil
become progressively more severe. Hence, because of viscous effects, a
smaller proportion of the theoretical design negative load is realized
near the trailing edge so that the amount of effective positive camber
is increased and thus the angle of zero lift becomes more negative.

Drag

In order to show more clearly the effects of airfoil design on the
drag, the drag polars for the different airfoils are plotted together
in figures 12 and 13 for the smooth surface condition at a Reynolds
number of 2.6×10^6 and in figures 14 and 15 for the rough surface
condition at a Reynolds number of 2.1×10^6. Figures 12 and 14 show
the effects of varying camber on the drag characteristics of the airfoils
of 12-percent thickness, and figures 13 and 15 show the effects of
varying thickness ratio on the airfoils with design lift coefficient
of 0.5. The characteristics of the NACA 8-H-12 airfoil section, taken
from reference 3, are shown in the figures for comparison. The drag
characteristics that are discussed are: the minimum drag, the low-drag
range, the drag outside the low-drag range, and the maximum value of
the lift-drag ratio.

Minimum drag coefficient.- An examination of the data of figures 12
and 13 indicates that the values of the minimum drag coefficient for the

smooth condition at a Reynolds number of 2.6×10^6 range between 0.0045
and 0.0053 for the NACA 8-H-12 airfoil and all the airfoils of the pre-
sent investigation except for the highest-cambered section which had a
minimum drag coefficient of 0.0072. By way of comparison, the minimum
drags of the NACA 64_1-012 and NACA 23012 airfoil sections at a Reynolds
number of 3.0×10^6 are 0.0050 and 0.0064, respectively (reference 1).
The data of figures 12 and 13 clearly show that the value of the minimum
drag coefficient of the helicopter-rotor-blade sections is little
affected by the airfoil thickness but increases significantly with
camber. This significant effect of camber is contrary to previously
reported results (reference 1) that show that the magnitude of the
minimum drag coefficient is relatively insensitive to variations in the
amount of camber for NACA 6-series airfoil sections with the a = 1.0
type of mean line. The increase of minimum drag with camber shown by
the H-series sections probably can be explained by the fact that the
pressure gradient over the forward part of the upper surface becomes
increasingly unfavorable to laminar flow as the camber increases
(figs. 3, 4, and 5).

The effect of Reynolds number on the minimum drag can be seen in
figures 7 to 11. In general, increasing the Reynolds number
from 0.9×10^6 to 2.1×10^6 appears to have a rather important favorable
effect upon the minimum drag. This trend is particularly pronounced for
the thicker, more highly cambered sections. The existence at the lower
Reynolds number of a large separation bubble on the upper surface that
decreases rapidly in size as the Reynolds number is increased
to 2.1×10^6 may possibly account for the large favorable scale effect.
Further increases in the Reynolds number to 2.6×10^6 appear to have a
relatively unimportant and seemingly inconsistent effect upon the
minimum drag. The small amount of adverse scale effect shown by some of
the airfoils as compared with the favorable effect shown by others can,
however, be explained by the relation between the pressure gradient on
the upper surface of the airfoil and the critical boundary-layer
Reynolds number for transition. (See, for example, reference 7.)

The effect of leading-edge roughness is to increase greatly the
minimum drag of all the airfoils (figs. 14 and 15). Variations in the
airfoil thickness from 9 to 12 percent of the chord and in the amount
of camber from theoretical design lift coefficients of 0.3 to 0.5 had
little effect on the minimum drag that was of the order of 0.012. For
the 15-percent-thick airfoil and the airfoil with 0.7 design lift
coefficient, however, the value of the minimum drag is of the order
of 0.015. The minimum drag coefficient of the NACA 8-H-12 airfoil
section (with roughness) at a Reynolds number of 2.1×10^6 is approxi-
mately 0.0104. Unpublished data indicate that NACA 6-series

and 230-series airfoils of 12-percent to 15-percent thickness have
minimum drag for the rough condition of about 0.012 at a corresponding
Reynolds number.

Low-drag range.- Because of the similar pressure gradients on the
upper and lower surfaces of conventional NACA 6-series airfoils at the
design condition, the theoretical design lift coefficients for these
airfoils usually occur near the experimentally determined center of
that range of lift coefficient through which low drag is obtained. At
the theoretical design lift coefficient, the pressure gradients on the
upper and lower surfaces of the NACA H-series airfoils, however, are
usually dissimilar, and therefore the theoretical value of the design
lift coefficient would not occur in the center of the low-drag range.
An examination of the pressure-distribution data of figures 2 to 6
indicates that, at the design lift coefficient, the pressure gradients
on the upper surface are generally much less favorable for the mainte-
nance of laminar flow than are those on the lower surface. A con-
sideration of this fact, together with a knowledge of the type of load
distribution due to angle of attack shown by the NACA 64-series basic
thickness form (reference 1), suggests that the theoretical design lift
coefficient of the NACA H-series airfoils should occur nearer the high
rather than the low end of the lift-coefficient range for low drag.
On the contrary, however, the theoretical value of the design lift
coefficient occurs closer to the lower end of the low-drag range
(figs. 12 and 13). This result can be explained in the following
qualitative manner:

As was pointed out in the discussion of the theoretical character-
istics of the H-series airfoils, the theoretical load distribution near
the trailing edge is probably not fully realized experimentally because
of the effects of viscosity. If such is the case, the pressure gradi-
ents on the forward portions of the upper and lower surfaces of the
H-series sections at the theoretical design lift coefficient actually
occur at a higher experimental lift coefficient because the load near
the trailing edge of these airfoils acts in a negative direction.
Hence, when the theoretical design lift coefficient is reached experi-
mentally, the pressure gradient on the lower surface would be much less
favorable to laminar flow than is indicated theoretically and a peak
would be expected to form near the leading edge as the lift coefficient
is reduced much below the theoretical design value. As a result,
turbulent flow would begin near the leading edge on the lower surface
and therefore the drag would rise rapidly. If this explanation of the
observed behavior of the design lift coefficient is correct, increasing
the design lift coefficient of the H-series sections would be expected
to cause the theoretical design lift coefficient to occur closer to the
lower end of the range of lift coefficient for low drag. The data of
figure 12 show that such is the case; in fact, for the highest-cambered
section, the theoretical design lift coefficient occurs below the lower

limit of the low-drag range. The experimentally observed shift of the
design lift coefficient to higher values was expected because of the
manner in which the estimated loss in load near the trailing edge was
accounted for so that the experimental pitching moments would be zero.

In spite of the fact that the lift coefficient corresponding to the
center of the low-drag range bears little relation to the theoretical
design lift coefficient, the designer is probably most interested in the
lift coefficient at the center of the low-drag range. The value of this
lift coefficient increases from approximately 0.4 to 1.0 as the theo-
retical design lift coefficient is increased from 0.3 to 0.7 (fig. 12).
The width of the low-drag range does not appear to vary appreciably with
the amount of camber, but as might be expected, it increases somewhat
with airfoil thickness (fig. 13). The data of figures 12 and 13 show
the NACA 8-H-12 section to have a more extensive low-drag range than
any of the airfoils of the present investigation. Because of the manner
in which the low-drag range increases with thickness, the value of the
lift coefficient corresponding to the center of this range also
increases somewhat with thickness. The values of the lift coefficient
corresponding to the center of the low-drag range for all the airfoils
are summarized in table VI.

Variations in the Reynolds number between 2.1×10^6 and 2.6×10^6
appear to have a relatively unimportant effect upon the low-drag range
(figs. 7 to 11). Lowering the Reynolds number to 0.9×10^6, however,
results in the almost complete disappearance of the low-drag "bucket"
for all the airfoils except the one of lowest camber. This disappear-
ance is believed to be associated with the existence of rather extensive
regions of laminar separation on the upper surfaces of the airfoils.

With standard leading-edge roughness no low-drag range exists, of
course, that corresponds to the attainment of extensive laminar layers
on either surface. The drag polars for the different airfoils in the
rough condition (figs. 14 and 15), however, do have a range of lift
coefficient through which the drag coefficient varies only slightly from
the minimum value. The data of figures 14 and 15 show that this range
decreases markedly with both increasing thickness and increasing camber
and that the center of this range generally bears little relation to the
center of the low-drag range obtained for the airfoils in the smooth
condition. These results can possibly be explained by the fact that the
pressure-recovery gradients on the upper surfaces of the airfoils become
increasingly more severe as the thickness and camber are increased and,
hence, separation of the turbulent boundary layer is promoted. In
comparison with the airfoils of the present investigation, the
NACA 8-H-12 airfoil appears to have drag near the minimum value in the
rough condition over an extremely wide range of lift coefficient
(figs. 14 and 15).

Drag outside the low-drag range.- As the lift coefficient is decreased below those values corresponding to the lower end of the low-drag range, the drag of all the smooth airfoils first rises abruptly, then rather slowly, then very abruptly again (figs. 12 and 13). The same type of "jog" appears in the polars for some of the airfoils following the upper end of the low-drag range, and in all cases, the drag finally rises abruptly. The exact extent and the nature of these jogs vary somewhat with the airfoil design parameters. The net effect is that the lift-coefficient range between the final abrupt rise in drag on the two sides of the polar increases with airfoil thickness and decreases somewhat with camber. The NACA 8-H-12 airfoil appears to have a wider range of lift coefficient between the two abrupt increases in drag than do any of the airfoils of the present investigation (figs. 12 and 13).

In the rough condition, the rate of drag rise above the flat portion of the polar is very steep and in general does not appear to vary with airfoil thickness and camber (figs. 14 and 15).

Maximum lift-drag ratios.- The values of the maximum section lift-drag ratio are included in table VI for the airfoils of the present investigation and for the NACA 8-H-12 and 23012 sections. For the smooth surface condition, the maximum values of the lift-drag ratio at a Reynolds number of 2.6×10^6 vary between 147 and 153 for all the airfoils of the present investigation except for the 12-percent-thick section with the smallest design lift coefficient, 0.3. The maximum value of the lift-drag ratio for both this airfoil and the NACA 8-H-12 airfoil was of the order of 135. In comparison with the value of 111 obtained for the NACA 23012 section (reference 1), the lift-drag ratios of the newer sections seem quite high. Variations in the Reynolds number between 2.6×10^6 and 2.1×10^6 had a somewhat inconsistent effect upon the value of the lift-drag ratio for the different airfoils (table VI), whereas decreasing the Reynolds number to 0.9×10^6 caused reductions in the lift-drag ratios in all cases.

The addition of standard leading-edge roughness caused large decreases in the value of the lift-drag ratio for all the airfoils, the amount of the decrement increasing with both airfoil thickness and camber. In the rough condition, the NACA 8-H-12 section has a value of the lift-drag ratio higher than that of any of the airfoils of the present investigation. Unpublished data show that at a Reynolds number of 2.0×10^6 the value of the maximum lift-drag ratio for the NACA 23012 section in the rough condition is 45, which is higher than that of many of the newer airfoils.

HELICOPTER PERFORMANCE CALCULATIONS

Although the preceding discussion of the effect of airfoil design upon the section aerodynamic characteristics of the airfoils may be of interest, their merits may be adequately judged only through a consideration of the relative performance of helicopter rotors employing the different sections. A method of evaluating the relative performance that can be expected for various flight conditions as a result of employing different airfoil sections in a rotor consists of predicting the power that will be expended in overcoming the rotor-blade profile drag. This method of analysis was dealt with in reference 4 and the nondimensional weighting curves developed in that paper have been used for calculating and comparing the profile-drag power losses that result when the airfoils of the present investigation are incorporated in sample rotors. The calculations have been made for the various configurations and flight conditions covered in the original analysis (reference 4).

A list of the flight conditions and assumed characteristics of the sample helicopter is given in table VII. The results of the calculations are presented in table VIII for smooth and rough airfoil surface conditions, and values taken from reference 3 are included for the NACA 8-H-12 and 23012 airfoil sections.

It should be noted that the method of analysis employed makes the simplifying assumption that section characteristics corresponding to a single Reynolds number apply for the entire rotor disk; whereas in the case of the assumed rotor, the variation of the Reynolds number is between zero and approximately 4×10^6 for a tip-speed ratio of 0.2 (reference 4). Good agreement between predictions made by the theory discussed in reference 4 and experiment is indicated, however, in reference 8. In the present calculations, section data corresponding to a Reynolds number of 2.6×10^6 were employed in all cases. This mean value is the same as that employed in reference 4 for rotors having the same maximum Reynolds number at the tip as do those considered in the present calculations.

A comparison of the results in table VIII indicates that, for the smooth surface condition, the NACA 11-H-09 airfoil is the best of the five airfoils tested in the present investigation for nearly all the flight conditions investigated. The gains to be expected by using the NACA 11-H-09 section in preference to one of the others varies, however, to a large extent with the flight condition. The results also indicate that the NACA 11-H-09 section is about equally as good as the NACA 8-H-12 section at the conditions of high disk loading and high tip-speed ratio. For the other conditions considered, however, the

NACA 8-H-12 section shows smaller losses than were calculated for the
NACA 11-H-09 section. The NACA 8-H-12 and 11-H-09 airfoils both show
net power savings for most of the flight conditions when considered in
relation to the NACA 23012 airfoil. The NACA 23012 airfoil, however,
appears to be better than the other airfoils of the present investi-
gation for many individual flight conditions. Variations in airfoil
thickness and camber have an appreciable effect upon the drag power;
however, the amount and direction of the effect seem to vary markedly
with the flight condition being considered.

As an aid in understanding the reason that different airfoils may
be preferred for applications emphasizing different flight conditions,
a few sample weighting curves (taken from reference 4) showing the
relative distribution of profile-drag power for different helicopter
operating conditions are presented in figure 16. The weighting curves
are presented for tip-speed ratios of 0 (hovering), 0.2, and 0.3.
These curves show, for example, that both the small range of angle of
attack over which the largest power losses occur and the entire range
of angle of attack which need be considered vary with the operating
condition. The application of two of the weighting curves in calcu-
lating the distribution of profile-drag power loss for the NACA 8-H-12
and 11-H-09 airfoil sections is shown in figure 17. The curves of
figure 17 were obtained by multiplying the drag polars of the two
airfoils by the weighting curves of figure 16 for tip-speed ratios
of 0.2 and 0.3. Since the area under each curve of figure 17 represents
the total profile-drag power loss, the influence of different regions
of the drag polars for these airfoils on the magnitude of the total
power loss is indicated for the operating conditions considered.

In the rough leading-edge condition, the data of table VIII again
show the NACA 11-H-09 section to be the best of the airfoils considered
in the present investigation for most flight conditions, although in
many cases the results for this airfoil do not differ much from those
for the 12-percent-thick section of smallest camber. In general, the
results for the NACA 8-H-12 section are similar to those for the
NACA 11-H-09 section. The data for the airfoils in the rough condition
are rather consistent in that they show the profile-drag power loss to
increase in all cases with increasing airfoil thickness and camber.
The amount of the increase, however, depends markedly on the flight
condition, although in general, increasing the camber of the 12-percent-
thick section has a less adverse effect than increasing the thickness
from 9 to 15 percent with constant camber of 0.5 design lift coefficient.

CONCLUSIONS

A two-dimensional wind-tunnel investigation has been made of five NACA airfoils of varying thickness and camber designed for use in rotor blades. For the range of values of thickness and camber covered, the following conclusions can be drawn from the results of the investigation:

1. Near-zero pitching moments about the aerodynamic center were obtained for all the airfoils in the useful range of lift coefficient. The position of the aerodynamic center did not vary appreciably with airfoil thickness and camber.

2. The values of the maximum lift coefficient for the smooth condition in most cases showed little variation with airfoil thickness and camber and were in general lower than those for symmetrical NACA 64-series airfoils of corresponding thickness. In the rough surface condition, the maximum lift decreased, although in a not entirely consistent manner, with both increasing thickness and camber.

3. The value of the minimum drag coefficient for the smooth surface condition increased significantly with camber but was little affected by variations in the airfoil thickness. With roughened leading edges, the value of the minimum drag seemed to be relatively insensitive to variations in thickness and camber in most cases.

4. In the smooth surface condition, the value of the lift coefficient corresponding to the center of that range of lift coefficient through which low drag prevails increased with increasing camber and, in all cases, was larger than the theoretical design lift coefficient. Increasing the airfoil thickness caused some increase in the low-drag range. In the rough surface condition, increases in both camber and thickness had a very adverse effect upon the drag polar in all cases.

5. For various flight conditions, comparisons of the predicted relative performance of sample helicopter rotors employing the different airfoil sections indicate that, in general, the NACA 11-H-09 airfoil is the best airfoil of the group investigated for both smooth and rough surface conditions. The effect of increasing airfoil thickness and camber upon the relative performance varied with the flight condition for the smooth airfoils, but in all cases, increases in thickness and camber had an adverse effect upon performance when the airfoil surfaces were rough.

6. In comparison with the NACA 8-H-12 airfoil (designed in a previous NACA investigation), the NACA 11-H-09 airfoil does not appear to offer any hope of gains in performance for most of the flight

conditions considered. Both the NACA 8-H-12 and 11-H-09 airfoil
sections show net power savings in comparison with the NACA 23012 air-
foil for most of the flight conditions, whereas the NACA 23012 airfoil
appears to be better than the other airfoils of the present investiga-
tion in most cases.

Langley Aeronautical Laboratory
     National Advisory Committee for Aeronautics
          Langley Air Force Base, Va., June 1, 1949

REFERENCES

1. Abbott, Ira H., Von Doenhoff, Albert E., and Stivers, Louis S., Jr.:
     Summary of Airfoil Data. NACA Rep. 824, 1945.

2. Tetervin, Neal: Tests in the NACA Two-Dimensional Low-Turbulence
     Tunnel of Airfoil Sections Designed to Have Small Pitching
     Moments and High Lift-Drag Ratios. NACA CB 3I13, 1943.

3. Stivers, Louis S., Jr., and Rice, Fred J., Jr.: Aerodynamic
     Characteristics of Four NACA Airfoil Sections Designed for
     Helicopter Rotor Blades. NACA RB L5K02, 1946.

4. Gustafson, F. B.: Effect on Helicopter Performance of Modifications
     in Profile-Drag Characteristics of Rotor-Blade Airfoil Sections.
     NACA ACR L4H05, 1944.

5. Von Doenhoff, Albert E., Stivers, Louis S., Jr., and O'Connor,
     James M.: Low-Speed Tests of Five NACA 66-Series Airfoils Having
     Mean Lines Designed to Give High Critical Mach Numbers. NACA
     TN 1276, 1947.

6. Von Doenhoff, Albert E., and Abbott, Frank T., Jr.: The Langley Two-
     Dimensional Low-Turbulence Pressure Tunnel. NACA TN 1283, 1947.

7. Loftin, Laurence K., Jr., and Cohen, Kenneth S.: Aerodynamic
     Characteristics of a Number of Modified NACA Four-Digit-Series
     Airfoil Sections. NACA TN 1591, 1948.

8. Gustafson, F. B., and Gessow, Alfred: Effect of Blade Stalling on
     the Efficiency of a Helicopter Rotor as Measured in Flight.
     NACA TN 1250, 1947.

TABLE I.- ORDINATES FOR
NACA 11-H-09 AIRFOIL SECTION

[Stations and ordinates given in
percent of airfoil chord]

Upper surface		Lower surface	
Station	Ordinate	Station	Ordinate
0	0	0	0
.134	.983	.866	-.301
.338	1.267	1.162	-.315
.785	1.745	1.715	-.311
2.000	2.660	3.000	-.238
4.475	3.996	5.525	-.090
6.988	5.018	8.012	.036
9.520	5.851	10.480	.135
14.615	7.112	15.385	.250
19.728	7.994	20.272	.278
24.844	8.569	25.156	.235
29.957	8.890	30.043	.144
35.075	8.975	34.925	.019
40.217	8.828	39.783	-.142
45.331	8.387	44.669	-.315
50.394	7.721	49.606	-.513
55.410	6.898	54.590	-.710
60.392	5.967	59.608	-.893
65.352	4.963	64.648	-1.047
70.295	3.915	69.705	-1.173
75.226	2.862	74.774	-1.252
80.151	1.843	79.849	-1.271
85.080	.916	84.920	-1.216
90.024	.170	89.976	-1.052
94.995	-.271	95.005	-.725
100.000	0	100.000	0

L.E. radius: 0.579
Slope of radius through L.E.: 0.569

TABLE II.- ORDINATES FOR
NACA 12-H-12 AIRFOIL SECTION

[Stations and ordinates given in
percent of airfoil chord]

Upper surface		Lower surface	
Station	Ordinate	Station	Ordinate
0	0	0	0
.183	1.123	.817	-.727
.392	1.403	1.108	-.843
.850	1.862	1.650	-1.008
2.061	2.723	2.939	-1.251
4.521	3.990	5.479	-1.548
7.012	4.975	7.988	-1.743
9.515	5.800	10.485	-1.882
14.564	7.102	15.436	-2.096
19.640	8.074	20.360	-2.246
24.729	8.778	25.271	-2.360
29.829	9.246	30.171	-2.438
34.957	9.472	35.043	-2.484
40.154	9.433	39.846	-2.525
45.303	9.048	44.697	-2.532
50.391	8.412	49.609	-2.520
55.425	7.591	54.575	-2.485
60.422	6.634	59.578	-2.422
65.389	5.583	64.611	-2.327
70.330	4.466	69.670	-2.202
75.252	3.333	74.748	-2.033
80.166	2.230	79.834	-1.814
85.085	1.219	84.915	-1.539
90.024	.387	89.976	-1.185
94.994	-.150	95.006	-.726
100.000	0	100.000	0

L.E. radius: 1.040
Slope of radius through L.E.: 0.343

TABLE III.- ORDINATES FOR
NACA 13-H-12 AIRFOIL SECTION

[Stations and ordinates given in
percent of airfoil chord]

Upper surface		Lower surface	
Station	Ordinate	Station	Ordinate
0	0	0	0
.025	1.183	.975	-.527
.213	1.511	1.287	-.589
.642	2.057	1.858	-.663
1.820	3.110	3.180	-.726
4.268	4.674	5.732	-.752
6.772	5.883	8.228	-.747
9.299	6.882	10.701	-.732
14.410	8.426	15.590	-.738
19.553	9.535	20.447	-.773
24.708	10.296	25.292	-.840
29.867	10.757	30.133	-.927
35.045	10.929	34.955	-1.027
40.282	10.794	39.718	-1.154
45.455	10.284	44.545	-1.276
50.555	9.501	49.445	-1.403
55.588	8.521	54.412	-1.523
60.574	7.395	59.426	-1.629
65.523	6.172	64.477	-1.706
70.440	4.889	69.560	-1.753
75.335	3.596	74.665	-1.752
80.220	2.350	79.780	-1.684
85.114	1.220	84.886	-1.534
90.034	.306	89.966	-1.264
94.993	-.257	95.007	-.833
100.000	0	100.000	0

L.E. radius: 1.040
Slope of radius through L.E.: 0.556

NACA

TABLE IV.- ORDINATES FOR
NACA 14-H-12 AIRFOIL SECTION

[Stations and ordinates given in
percent of airfoil chord]

Upper surface		Lower surface	
Station	Ordinate	Station	Ordinate
0	0	0	0
-.096	1.233	1.096	-.319
.071	1.606	1.429	-.322
.469	2.237	2.031	-.301
1.608	3.478	3.392	-.180
4.033	5.338	5.967	.062
6.543	6.774	8.457	.262
9.089	7.952	10.911	.428
14.257	9.746	15.743	.626
19.466	10.994	20.534	.704
24.686	11.812	25.314	.678
29.905	12.269	30.095	.583
35.133	12.384	34.867	.430
40.409	12.152	39.591	.218
45.606	11.515	44.394	-.017
50.717	10.585	49.283	-.281
55.750	9.444	54.250	-.556
60.725	8.150	59.275	-.830
65.650	6.758	64.344	-1.082
70.549	5.307	69.451	-1.303
75.416	3.857	74.584	-1.469
80.274	2.470	79.726	-1.550
85.143	1.223	84.857	-1.527
90.043	.225	89.957	-1.345
94.992	-.363	95.008	-.939
100.000	0	100.000	0

L.E. radius: 1.040
Slope of radius through L.E.: 0.768

TABLE V.- ORDINATES FOR
NACA 15-H-15 AIRFOIL SECTION

[Stations and ordinates given in
percent of airfoil chord]

Upper surface		Lower surface	
Station	Ordinate	Station	Ordinate
0	0	0	0
-.062	1.382	1.062	-.756
.114	1.750	1.386	-.870
.515	2.354	1.985	-1.024
1.633	3.537	3.367	-1.213
4.000	5.335	6.000	-1.381
6.455	6.774	8.545	-1.444
8.976	7.990	11.024	-1.476
14.054	9.913	15.946	-1.501
19.247	11.348	20.753	-1.524
24.475	12.354	25.525	-1.576
29.724	12.981	30.276	-1.647
35.001	13.241	34.999	-1.723
40.386	13.089	39.614	-1.837
45.669	12.451	44.331	-1.935
50.833	11.472	49.167	-2.046
55.887	10.250	54.113	-2.156
60.856	8.856	59.144	-2.252
65.767	7.353	64.233	-2.317
70.633	5.789	69.367	-2.339
75.474	4.230	74.526	-2.294
80.310	2.739	79.690	-2.165
85.159	1.391	84.841	-1.947
90.044	.311	89.956	-1.587
94.987	-.339	95.013	-1.031
100.000	0	100.000	0

L.E. radius: 0.382
Slope of radius through L.E.: 0.525

NACA

TABLE VI.- AIRFOIL SECTION CHARACTERISTICS

| NACA airfoil section | $(c_l/c_d)_{max}$ | | | $c_{l_{max}}$ | | | $c_{d_{min}}$ | | | c_{mac} $(R\approx2.6\times10^6)$ (a) | Low-drag range $(R\approx2.6\times10^6)$ | c_{l_i} (exp.) $(R\approx2.6\times10^6)$ | M_{cr} | | t/c at 0.25c | Aerodynamic-center position | |
| | Smooth | | Rough $(R\approx2.1\times10^6)$ | Smooth | | Rough $(R\approx2.1\times10^6)$ | Smooth | | Rough $(R\approx2.1\times10^6)$ | | | | at c_{l_i} (b) | for basic symmetrical section, $c_l = 0$ | | x/c | y/c |
	$(R\approx2.1\times10^6)$	$(R\approx2.6\times10^6)$		$(R\approx2.1\times10^6)$	$(R\approx2.6\times10^6)$		$(R\approx2.1\times10^6)$	$(R\approx2.6\times10^6)$									
11-H-09	147	147	54	1.32	1.30	1.19	0.0047	0.0054	0.0113	0.005	0.58 to 0.79	0.68	0.580	0.784	0.083	0.280	0.056
12-H-12	149	133	47	1.26	1.28	1.17	.0050	.0045	.0118	.007	.26 to .53	.39	.625	.744	.111	.265	.080
13-H-12	148	148	40	1.25	1.29	1.13	.0057	.0053	.0118	.007	.50 to .85	.68	.573	.744	.112	.264	.103
14-H-12	169	150	33	1.39	1.38	1.07	.0063	.0072	.0148	0	.90 to 1.08	.99	.518	.744	.112	.259	.081
15-H-15	147	153	26	1.31	1.27	1.04	.0055	.0053	.0151	.006	----------	----	.547	.704	.140	.264	.087
c8-H-12 (reference 3)	130	135	62	1.25	1.26	1.11	.0047	.0046	.0104	.005	.25 to .91	.57	.569	-----	.117	.278	.020
d23012 (reference 1)	---	111	--	----	1.61	----	------	.0064	------	-.013	----------	----	.60	-----	.118	.241	.035

aValues are given for the smooth condition unless otherwise specified.

bMcr is given at the theoretical value of c_{l_i} for the airfoils of this investigation and the NACA 23012 airfoil, and at the experimental value of c_{l_i} for the NACA 8-H-12 airfoil.

cAll characteristics given for this airfoil at $R = 2.1 \times 10^6$ have been obtained by interpolation of the results at $R = 1.8 \times 10^6$ and $R = 2.6 \times 10^6$.

dAll experimental results for this airfoil are given for a Reynolds number of 3×10^6.

TABLE VII

FLIGHT CONDITIONS AND ASSUMED CHARACTERISTICS

OF THE SAMPLE HELICOPTER OF REFERENCE 4

[Rotor diam., 40 ft; tip speed, 400 fps;
gross weight for W/S of 2.5, 3140 lb]

Condition	μ	W/S	σ	θ_1	θ	λ	f
1	0	1.55	0.07	0	7	-------	15
2	0	3.33	.07	0	13	-------	15
3	0	5.42	.07	0	19	-------	15
4	0	2.5	.07	0	10.3	-------	15
5	.2	2.5	.07	0	9	-0.0385	15
6	.3	2.5	.07	0	11	-.0695	15
7	.2	1.9	.07	0	7	-.0319	15
8	.2	3.1	.07	0	11	-.0469	15
9	.2	2.5	.10	0	7	-.0350	15
10	.3	2.5	.07	-8	[a]10.5	-.0680	15

[a]Measured at 0.75 R.

TABLE VIII

COMPARISON OF ROTOR-BLADE PROFILE-DRAG LOSS FOR VARIOUS

FLIGHT CONDITIONS OF THE SAMPLE HELICOPTER

Helicopter conditions (see table VII)		Rotor-blade profile-drag loss, hp													Remarks
		NACA airfoil section													
		11-H-09		12-H-12		13-H-12		14-H-12		15-H-15		8-H-12 (a)		23012 (a)	
		Smooth	Rough	Smooth	Rough	Smooth	Rough	Smooth	Rough	Smooth	Rough	Smooth	Rough	Smooth	
1 $W/S = 1.55$	$\mu = 0$	21.8	34.4	13.5	35.8	22.3	37.3	30.9	45.7	25.4	50.5	14.4	32.3	20.1	Effect of loading (hovering flight)
2 $\quad\quad 3.33$	0	16.6	43.8	23.3	59.3	19.3	72.6	22.3	126.1	18.7	248.5	18.5	39.0	24.1	
3 $\quad\quad 5.42$	0	40.0	86.4	195.6	199.0	215.6	287.0	60.4	337.0	155.6	483.5	56.8	112.1	42.6	
4 $\mu = 0$	$W/S = 2.5$	16.7	36.8	17.7	40.6	16.2	45.6	25.2	64.9	17.9	153.8	16.3	35.3	21.7	Effect of tip-speed ratio
5 $\quad\quad .2$	2.5	23.1	44.8	32.1	60.9	30.1	74.6	29.5	103.3	26.3	181.2	21.2	41.4	25.7	
6 $\quad\quad .3$	2.5	32.0	60.5	58.7	81.9	66.5	101.9	57.7	134.2	63.8	194.2	36.7	65.7	31.0	
7 $W/S = 1.9$	$\mu = 0.2$	22.7	41.0	18.3	45.3	22.8	49.8	36.7	73.3	25.3	116.1	17.5	37.7	23.5	Effect of loading (forward flight)
5 $\quad\quad 2.5$	$.2$	23.1	44.8	32.1	60.9	30.1	74.6	29.5	103.3	26.3	181.2	21.2	41.4	25.7	
8 $\quad\quad 3.1$	$.2$	25.5	53.8	61.1	85.4	62.5	111.5	38.0	146.4	51.7	246.6	28.6	57.3	29.2	
5 $\sigma = 0.07$	$\mu = 0.2$	23.1	44.8	32.1	60.9	30.1	74.6	29.5	103.3	26.3	181.3	21.2	41.4	25.7	Effect of solidity
9 $\quad\quad .10$	$.2$	32.3	58.1	25.8	63.4	32.4	69.3	54.3	101.9	36.2	159.5	25.2	----	----	
6 $\theta_1 = 0°$	$\mu = 0.3$	32.0	60.5	58.7	81.9	66.5	101.9	57.7	134.2	63.8	194.2	36.7	65.7	31.0	Effect of blade twist
10 $\quad\quad -8°$	$.3$	29.2	53.7	44.5	71.0	50.3	86.6	54.9	120.7	46.5	170.6	27.7	----	----	

[a]From reference 3.

NACA
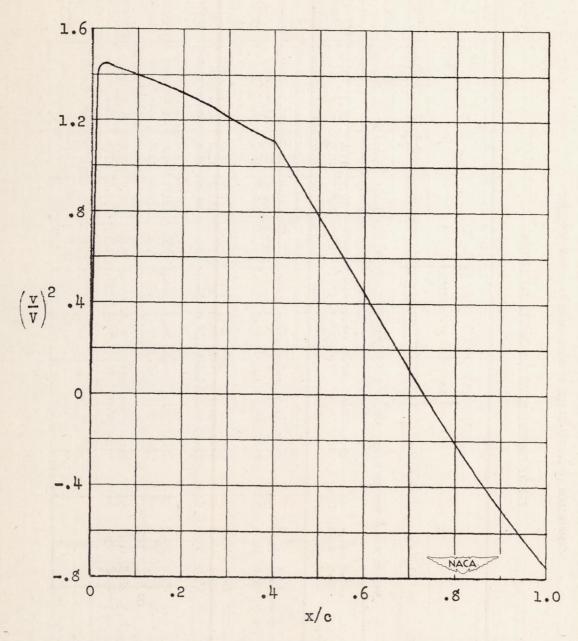
Figure 1.- Theoretical load distribution of the NACA 13-H-12 airfoil section at the design lift coefficient, $c_{l_i} = 0.5$.
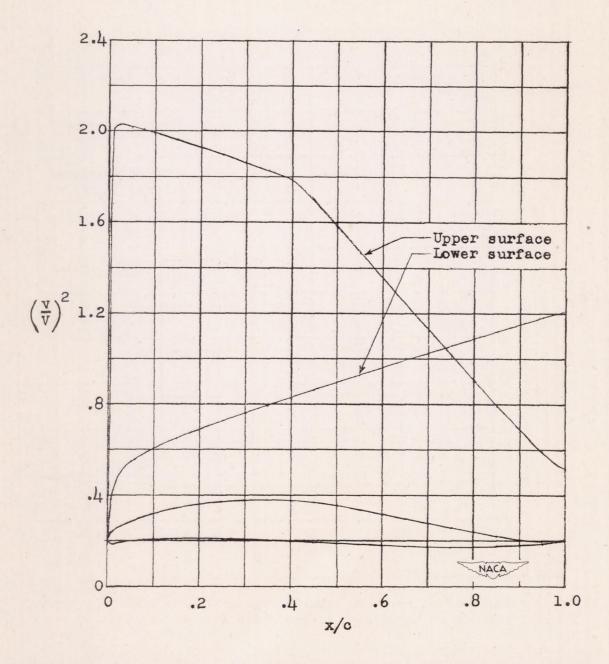
Figure 2.- Theoretical pressure distribution of the NACA 11-H-09 airfoil section at the design lift coefficient, $c_{l_i} = 0.5$.
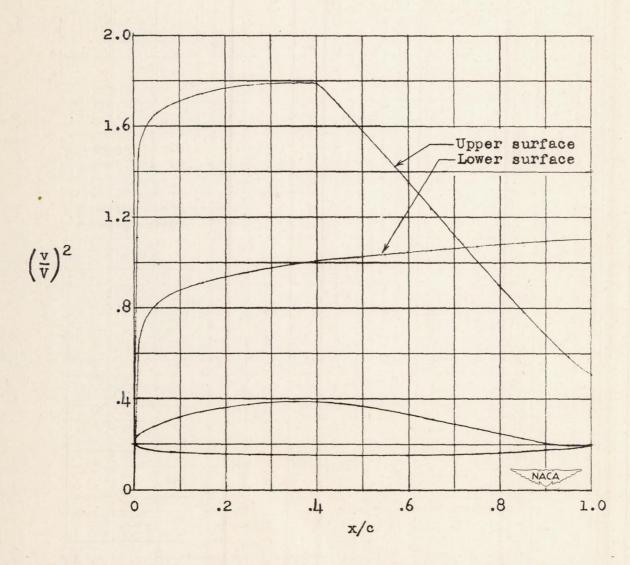
Figure 3.- Theoretical pressure distribution of the NACA 12-H-12 airfoil section at the design lift coefficient, $c_{l_i} = 0.3$.
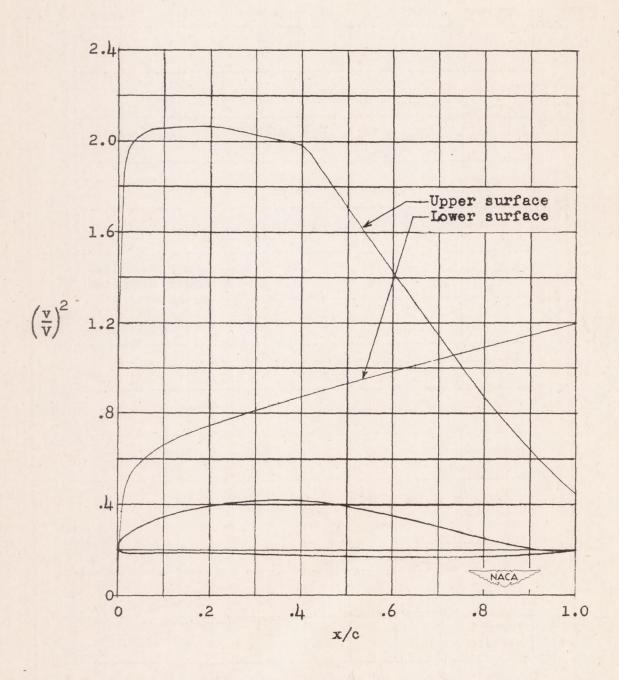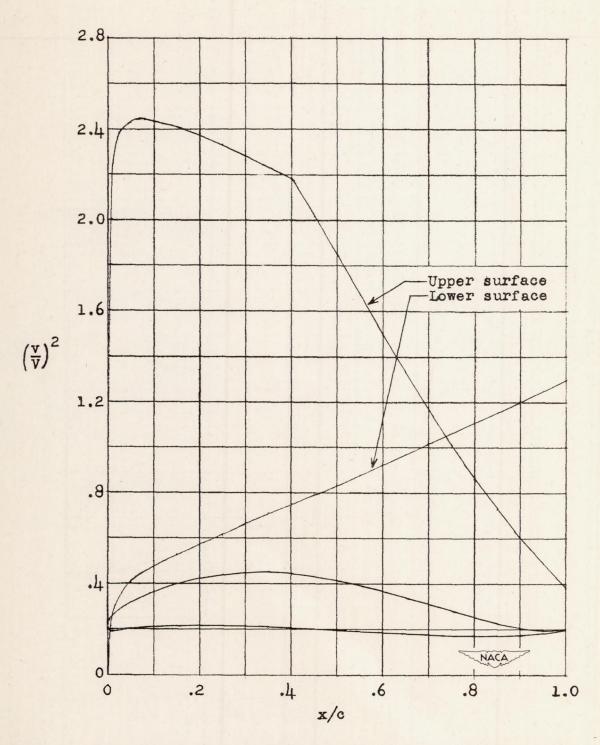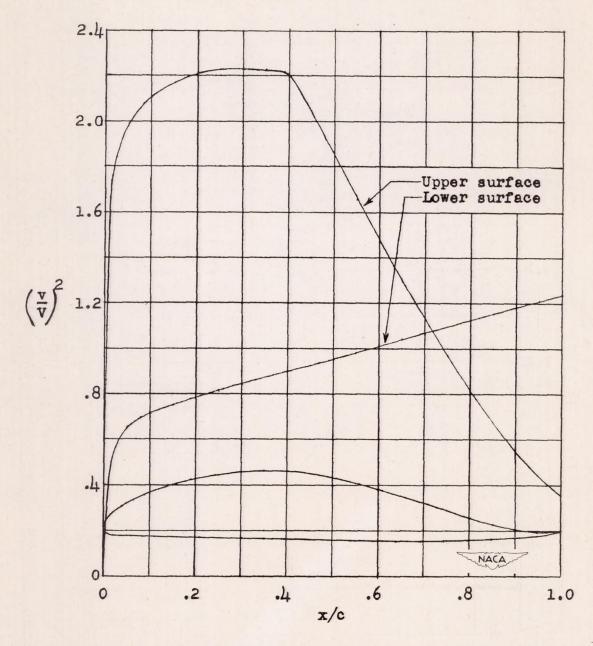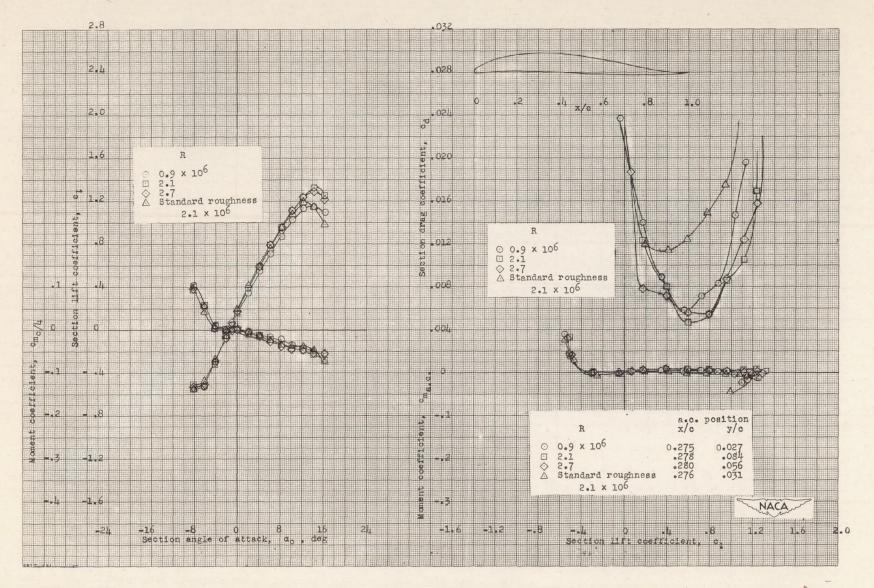
Figure 4.- Theoretical pressure distribution of the NACA 13-H-12 airfoil
section at the design lift coefficient, $c_{l_1} = 0.5$.

Figure 5.- Theoretical pressure distribution of the NACA 14-H-12 airfoil section at the design lift coefficient, $c_{l_i} = 0.7$.

Figure 6.- Theoretical pressure distribution of the NACA 15-H-15 airfoil section at the design lift coefficient, $c_{l_i} = 0.5$.

Figure 7.- Aerodynamic characteristics of the NACA 11-H-09 airfoil section, 24-inch chord.
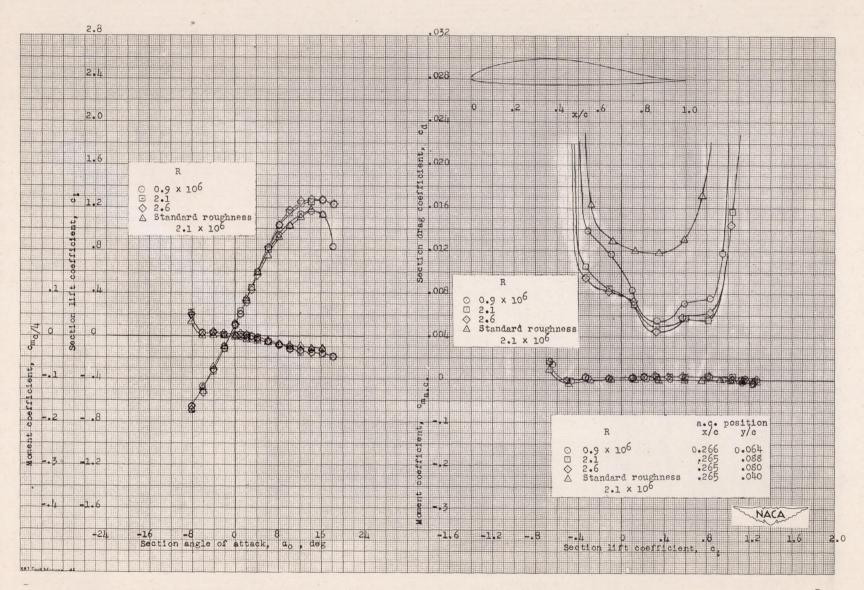
Figure 8.- Aerodynamic characteristics of the NACA 12-H-12 airfoil section, 24-inch chord.
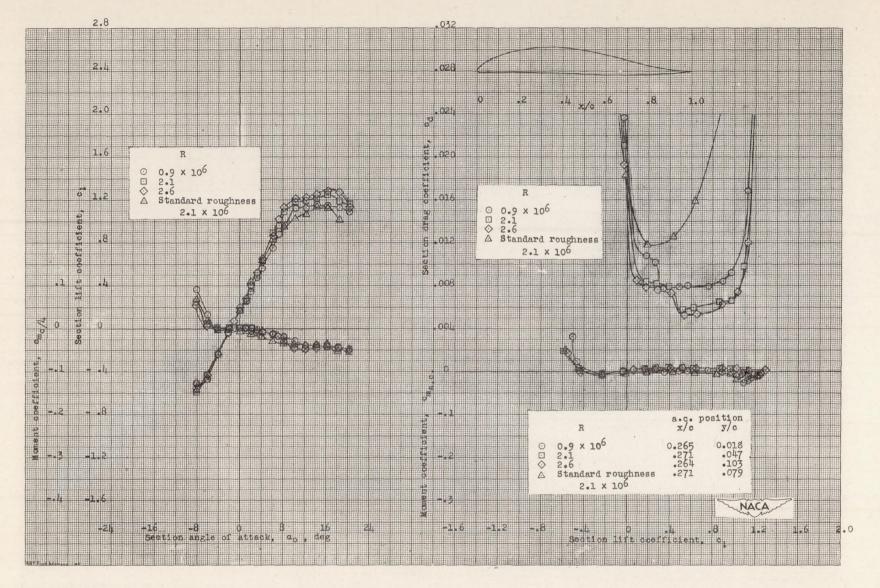
Figure 9.- Aerodynamic characteristics of the NACA 13-H-12 airfoil section, 24-inch chord.
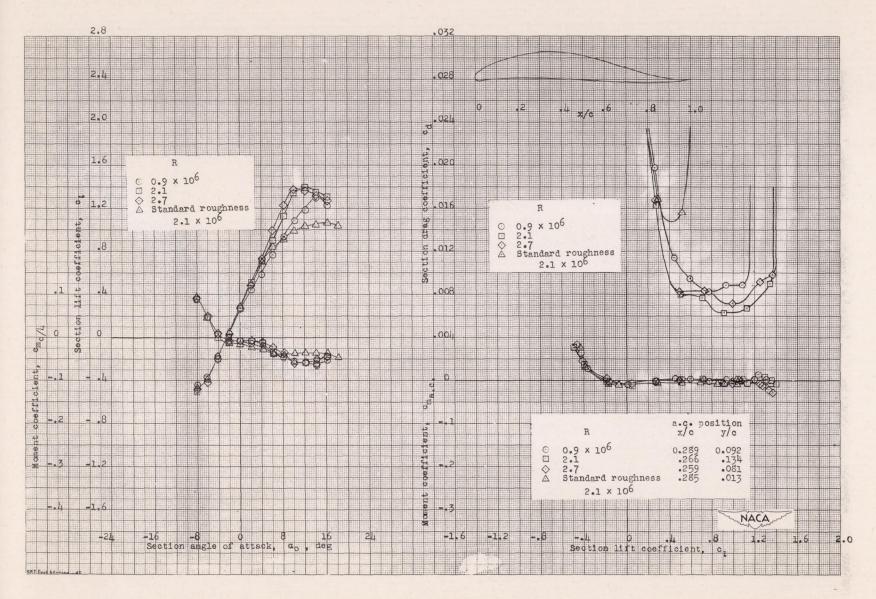
Figure 10.- Aerodynamic characteristics of the NACA 14-H-12 airfoil section, 24-inch chord.
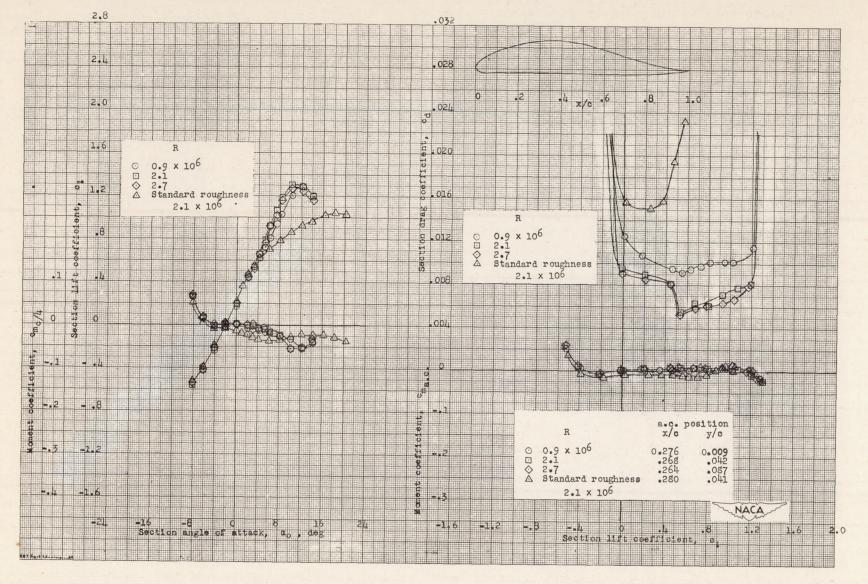
Figure 11.- Aerodynamic characteristics of the NACA 15-H-15 airfoil section, 24-inch chord.
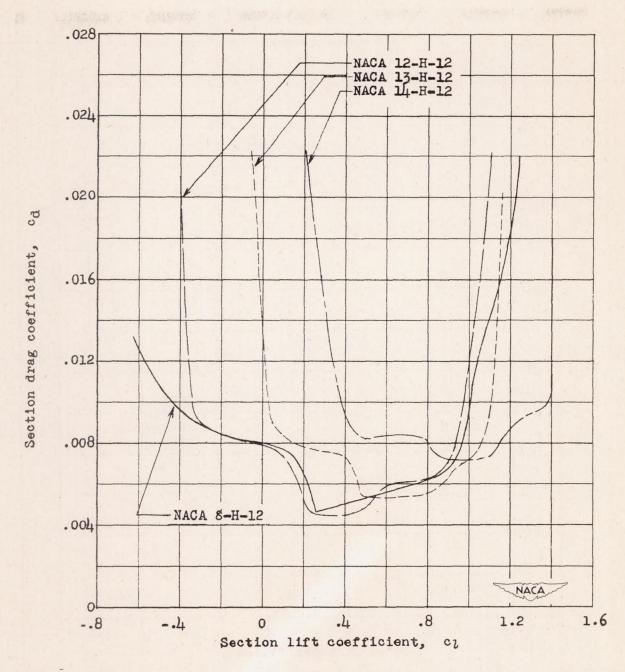
Figure 12.- Variation of section drag coefficient with section lift coefficient for the NACA 12-H-12, 13-H-12, and 14-H-12 airfoil sections. Smooth condition; $R = 2.6 \times 10^6$. Data for NACA 8-H-12 airfoil section are from reference 3.
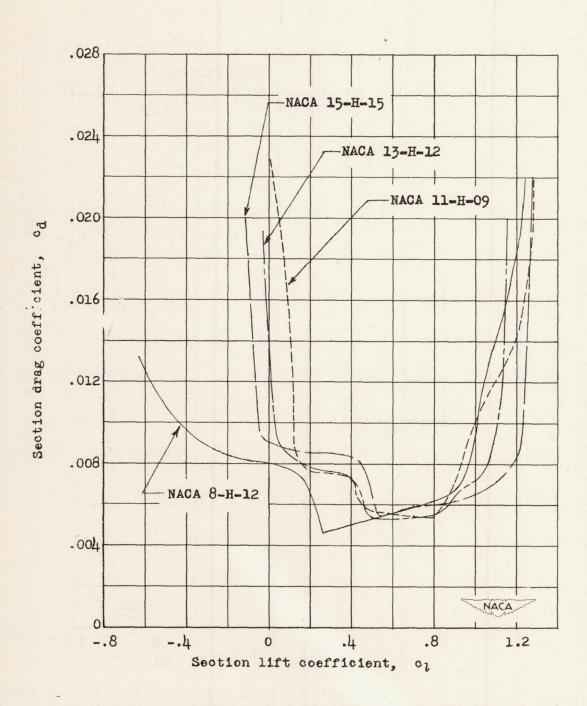
Figure 13.- Variation of section drag coefficient with section lift coefficient for the NACA 11-H-09, 13-H-12, and 15-H-15 airfoil sections. Smooth condition; $R = 2.6 \times 10^6$. Data for NACA 8-H-12 airfoil section are from reference 3.
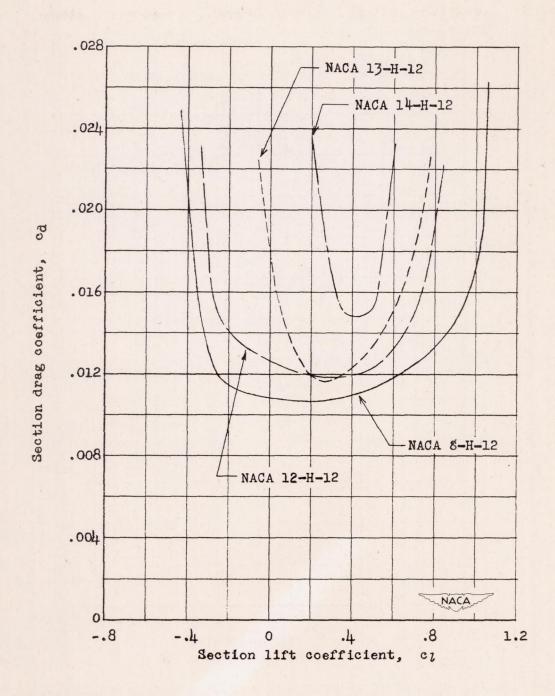
Figure 14.- Variation of section drag coefficient with section lift coefficient for the NACA 12-H-12, 13-H-12, and 14-H-12 airfoil sections with leading-edge roughness. $R = 2.1 \times 10^6$. Data for NACA 8-H-12 airfoil section are for $R = 1.8 \times 10^6$ (reference 3).
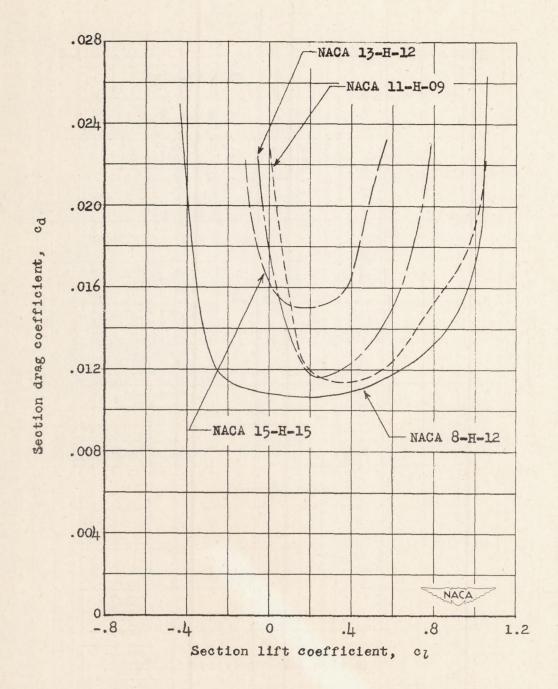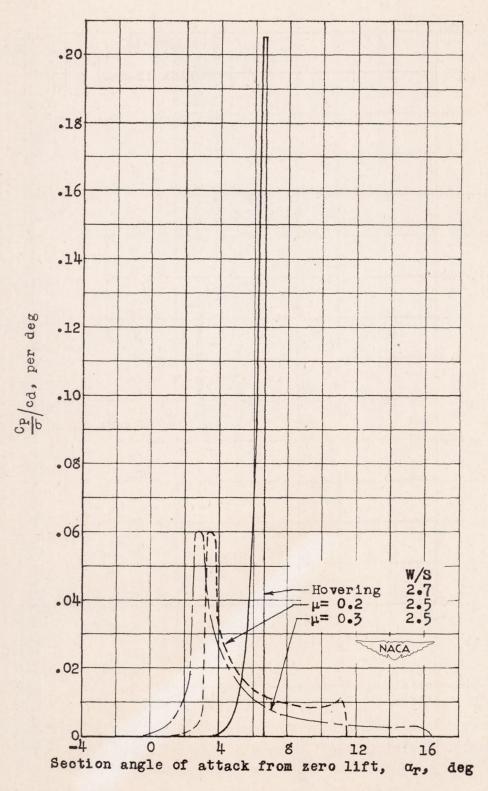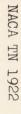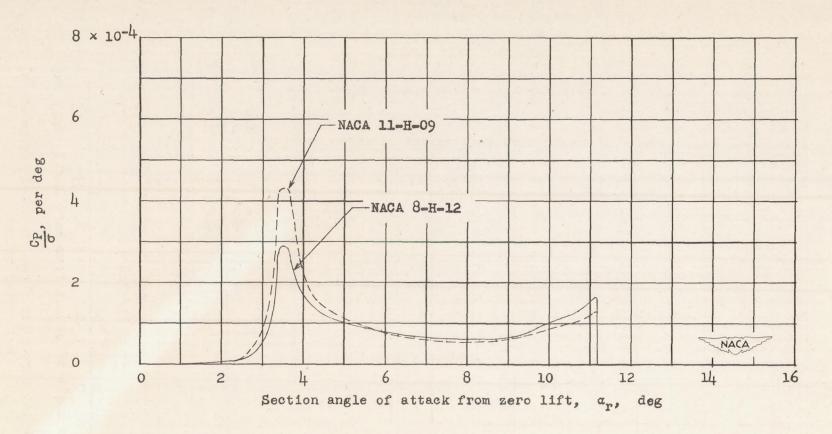
Figure 15.- Variation of section drag coefficient with section lift
coefficient for the NACA 11-H-09, 13-H-12, and 15-H-15 airfoil
sections with leading-edge roughness. $R = 2.1 \times 10^6$. Data for
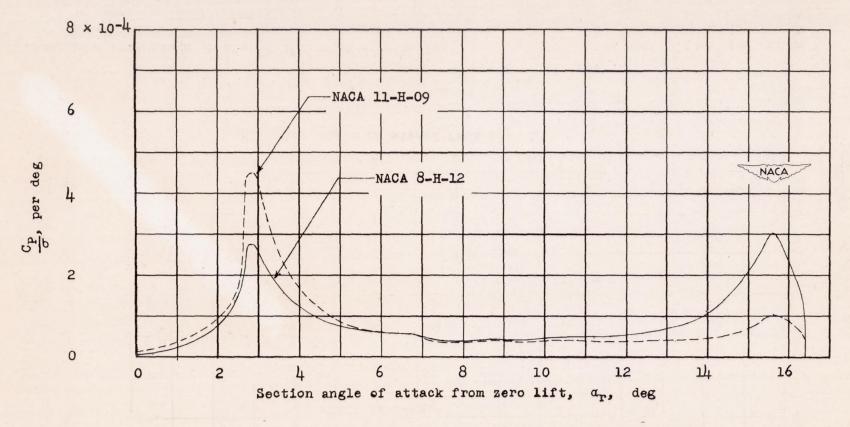NACA 8-H-12 airfoil section are for $R = 1.8 \times 10^6$ (reference 3).

Figure 16.- Weighting curves for three tip-speed ratios of the sample
helicopter rotor.

(a) $\mu = 0.2$; $\theta = 9°$; $\dfrac{W}{S} = 2.5$.

Figure 17.- Comparison of distributions of profile-drag power loss over the range of section angle of attack for the NACA 8-H-12 and 11-H-09 airfoil sections when used in the sample helicopter rotor. Smooth airfoil condition.

(b) $\mu = 0.3$; $\theta = 11°$; $\dfrac{W}{S} = 2.5$.

Figure 17.- Concluded.